Flinders
UNIVERSITY

DOI: http://dx.doi.org/10.1063/1.3230150

Cross sections for electron impact excitation of the C1Π and D1Σ+ electronic states in N2O

H. Kawahara, D. Suzuki, H. Kato, M. Hoshino, H. Tanaka et al.

Citation: J. Chem. Phys. **131**, 114307 (2009); doi: 10.1063/1.3230150
View online: http://dx.doi.org/10.1063/1.3230150
View Table of Contents: http://jcp.aip.org/resource/1/JCPSA6/v131/i11
Published by the American Institute of Physics.

Cross sections for electron impact excitation of the $C\ ^1\Pi$ and $D\ ^1\Sigma^+$ electronic states in N_2O

H. Kawahara,[1] D. Suzuki,[1] H. Kato,[1] M. Hoshino,[1] H. Tanaka,[1] O. Ingólfsson,[2] L. Campbell,[3] and M. J. Brunger[3,a)]
[1]*Department of Physics, Sophia University, Chiyoda-ku, Tokyo 102-8554, Japan*
[2]*Department of Chemistry, Science Institute, University of Iceland, Dunkaga 3, Reykjavík 107, Iceland*
[3]*ARC Centre for Antimatter-Matter Studies, School of Chemistry, Physics and Earth Sciences, Flinders University, GPO Box 2100, Adelaide, South Australia 5001, Australia*

(Received 17 June 2009; accepted 25 August 2009; published online 16 September 2009)

Differential and integral cross sections for electron-impact excitation of the dipole-allowed $C\ ^1\Pi$ and $D\ ^1\Sigma^+$ electronic states of nitrous oxide have been measured. The differential cross sections were determined by analysis of normalized energy-loss spectra obtained using a crossed-beam apparatus at six electron energies in the range 15–200 eV. Integral cross sections were subsequently derived from these data. The present work was undertaken in order to check both the validity of the only other comprehensive experimental study into these excitation processes [Marinković *et al.*, J. Phys. B **32**, 1949 (1998)] and to extend the energy range of those data. Agreement with the earlier data, particularly at the lower common energies, was typically found to be fair. In addition, the BE*f*-scaling approach [Kim, J. Chem. Phys. **126**, 064305 (2007)] is used to calculate integral cross sections for the $C\ ^1\Pi$ and $D\ ^1\Sigma^+$ states, from their respective thresholds to 5000 eV. In general, good agreement is found between the experimental integral cross sections and those calculated within the BE*f*-scaling paradigm, the only exception being at the lowest energies of this study. Finally, optical oscillator strengths, also determined as a part of the present investigations, were found to be in fair accordance with previous corresponding determinations. © *2009 American Institute of Physics*. [doi:10.1063/1.3230150]

I. INTRODUCTION

Nitrous oxide has been of interest to the broad scientific community for a number of years now, and for a very diverse range of reasons. These include its important role in the chemistry of the upper atmosphere where it is thought to contribute to the destruction of the ozone layer,[1] its use in several technological processes involving cold plasmas,[2] an astrophysical relevance due to both its detection in the star forming region Sgr B2(M) (Ref. 3), and as a component in interstellar ice.[4] It also has important applications in medicine, including its use in lasers and as a well known anesthetic.

Of particular interest to us is that N_2O is isoelectronic with CO_2. The dipole polarizabilities of the two molecules are very similar, [$\alpha(N_2O)=20\ a_0^3$ (Ref. 5)] and [$\alpha(CO_2)=19\ a_0^3$ (Ref. 6)], and both molecules are linear triatomics. CO_2 has no permanent dipole moment, while that for N_2O is very small [$\mu=0.16$ D (Ref. 7)]. Hence one might *a priori* expect that electron scattering behavior from the two species may be similar. As we have recently reported cross sections for electron impact excitation of the $^1\Sigma_u^+$ and $^1\Pi_u$ electronic states in CO_2,[8] the present study into excitation of the corresponding $^1\Sigma^+$ and $^1\Pi$ states of N_2O allows us to investigate that point.

There have been extensive studies for electron scattering from N_2O at the grand total cross section (TCS) level and for differential and integral cross sections for both elastic scattering and vibrational excitation. An excellent summary of that work is provided in Allan and Skalický,[9] to whom the interested reader is referred for more detail. With regard to cross section data for excitation of electronic states in N_2O, the work is much more limited with the most comprehensive experimental study being due to Marinković *et al.*[10] Here differential cross sections for both the $C\ ^1\Pi$ state (energy loss=8.5 eV) and $D\ ^1\Sigma^+$ state (energy loss=9.6 eV) were reported at energies of 20, 30, 50, and 80 eV and over the scattered electron angular range 10°–148°. A 1 keV study of the inelastic $X\ ^1\Sigma^+ \rightarrow D\ ^1\Sigma^+$ transition, for scattering at angles between 1.5°–10°, was reported by Boechat-Roberty *et al.*,[11] while an unpublished report from the 2007 International Conference on Photonic, Electronic, and Atomic Collisions (ICPEAC) meeting[12] described generalized oscillator strength measurements for both the $C\ ^1\Pi$ and $D\ ^1\Sigma^+$ states at an incident electron energy of 2500 eV.

From a theoretical perspective, it appears that the only major study available in the literature is a Schwinger variational iterative method (SVIM), in conjunction with a Born-closure approach, computation from Michelin *et al.*[13,14] Their differential cross sections (DCSs) and integral cross sections (ICSs), for energies in the range 10–80 eV, were reported for the excitation of the $C\ ^1\Pi$ state and a $^3\Pi$ state. A detailed comparison between the results of that calculation and the present and earlier data is made later in this paper.

In Sec. II we describe our experimental measurements and the generalized oscillator strength (GOS) analysis we

a)Electronic mail: michael.brunger@flinders.edu.au.

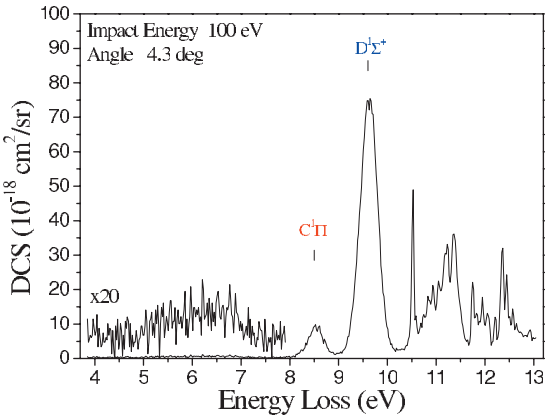

FIG. 1. Typical energy loss spectrum from the present study. The incident electron energy was $E=100$ eV, while the electron scattering angle was $\theta=4.3°$.

employed to derive the present ICSs and optical oscillator strengths, for both states. This is followed, for completeness, in Sec. III, by a very brief description of the BE*f*-scaling approach of Kim,[15] that we also employ here to calculate theoretical ICSs of the respective $C\ ^1\Pi$ and $D\ ^1\Sigma^+$ electronic states. In Sec. IV our results are presented and discussed with some conclusions from the current investigation being given in Sec. V.

II. EXPERIMENTAL AND ANALYSIS DETAILS

The present spectrometer[16] consists of an electron gun with a hemispherical monochromator, a nitrous oxide beam crossed at right angles to the incident electrons, and a rotable detector ($\theta_e=-10°-130°$) with a second hemispherical analyzer system. A number of electron optic elements image and energy-control the electron beam, with their performance having been checked by detailed electron trajectory calculations. Both the monochromator and analyzer are housed in differentially pumped boxes, in order to reduce the effect of any background gases and to minimize the stray electron background. The target molecular beam is produced by effusing N_2O through a simple nozzle with an internal diameter of 0.3 mm and a length of 5 mm.

The incident electron energies (E_0) of the present study were 15, 20, 30, 50, 100, and 200 eV, and the scattered electron angular range is 2°–130°. In all of these cases the energy resolution was in the range 35–40 meV [full width at half maximum (FWHM)] and the angular resolution was $\sim\pm1.5°$ (FWHM). The primary electron beam current was in the range 3–6 nA. Furthermore, the voltages for both the input and output lenses of the hemispheres were carefully adjusted to ensure that the base resolution of the energy loss spectra remained as symmetric as possible.

Energy loss spectra were measured, at each incident electron energy and each scattered electron angle, over the energy-loss range encompassing the elastic peak and from ~4–13 eV. A typical example of these data at $E_0=100$ eV and $\theta_e=4.3°$ is shown in Fig. 1, where we note that the elastic peak has been suppressed for the sake of clarity. The absolute scales (see the *y*-axis) of the present energy-loss spectra were set using the relative flow technique[17] with helium elastic DCSs as the standard.[18] Note that in each case it is the area under the $C\ ^1\Pi$ and $D\ ^1\Sigma^+$ energy-loss peaks that sets their respective differential cross sections, for the incident electron energy and electron scattering angle in question. For the incident energies of interest ($E_0=15-200$ eV) and the energy-loss range of interest ($\Delta E\approx0-10.3$ eV), the ratio of the energy loss to the incident energy varies roughly in the range of $0\leq\Delta E/E_0<0.69$. Thus it is crucial to establish the transmission of the analyzer over this energy-loss range, with our procedure for doing so being found in Kato *et al.*[19]

Experimental errors[20] on the present DCSs are estimated at about 20%, including components due to the uncertainty in our analyzer transmission response, an uncertainty due to errors associated with the elastic normalization cross sections and uncertainties due to any fluctuations in target density and/or the incident electron beam current during the measurements. The present experimental $C\ ^1\Pi$ and $D\ ^1\Sigma^+$ differential cross sections are plotted in Figs. 2 and 3 and tabulated in Tables I and II, with a full discussion of them being given later in Sec. IV of this paper.

The values of $[\theta_e,\mathrm{DCS}(\theta_e)]$ from our work, for each electronic state at each incident electron energy, are transformed to (K^2,G_{expt}) using the standard formula[15]

$$G_{\mathrm{expt}}(K^2)=\frac{(E/R)k_ia_0}{4a_0^2k_fa_0}K^2\mathrm{DCS}(E_0,\theta), \tag{1}$$

where k_i and k_f are the initial and final momenta of the incident and scattered electrons, E is the excitation energy for each electronic state, a_0 is the Bohr radius (0.529 Å), R is the Rydberg energy (13.6 eV), $G_{\mathrm{expt}}(K^2)$ is the experimental generalized oscillator strength, and K^2 is the momentum transfer squared defined by

$$K^2=(k_ia_0)^2+(k_fa_0)^2-2(k_ia_0)(k_fa_0)\cos\ \theta. \tag{2}$$

Vriens[21] proposed the following formula to represent the GOS for a dipole-allowed excitation based on the analytic properties identified by Lassettre[22] and Rau and Fano:[23]

$$G(x)=\frac{1}{(1+x)^6}\left[\sum_{m=0}^{\infty}\frac{f_mx^m}{(1+x)^m}\right], \tag{3}$$

where

$$x=\frac{K^2}{\alpha^2} \tag{4}$$

and

$$\alpha=\sqrt{B/R}+\sqrt{(B-E)/R}. \tag{5}$$

Note that in Eq. (5), B is the binding energy of the target electron.

In Eq. (3) the f_m are fitting constants to be determined in a least-squares fit analysis of the experimental GOSs, which via Eq. (1) are calculated from the DCSs of this study. Examples of the quality of those fits, for both the $C\ ^1\Pi$ and $D\ ^1\Sigma^+$ states, and for our $E_0=200$ eV data are given in Fig. 4. The beauty of Vriens'[21] formalism is that in principle at the $x=0$ optical limit, the value of $G(0)\equiv f_0$ is the optical oscillator strength (OOS). However, Lewis[24] recently commented that determining OOS from extrapolated GOSs, at

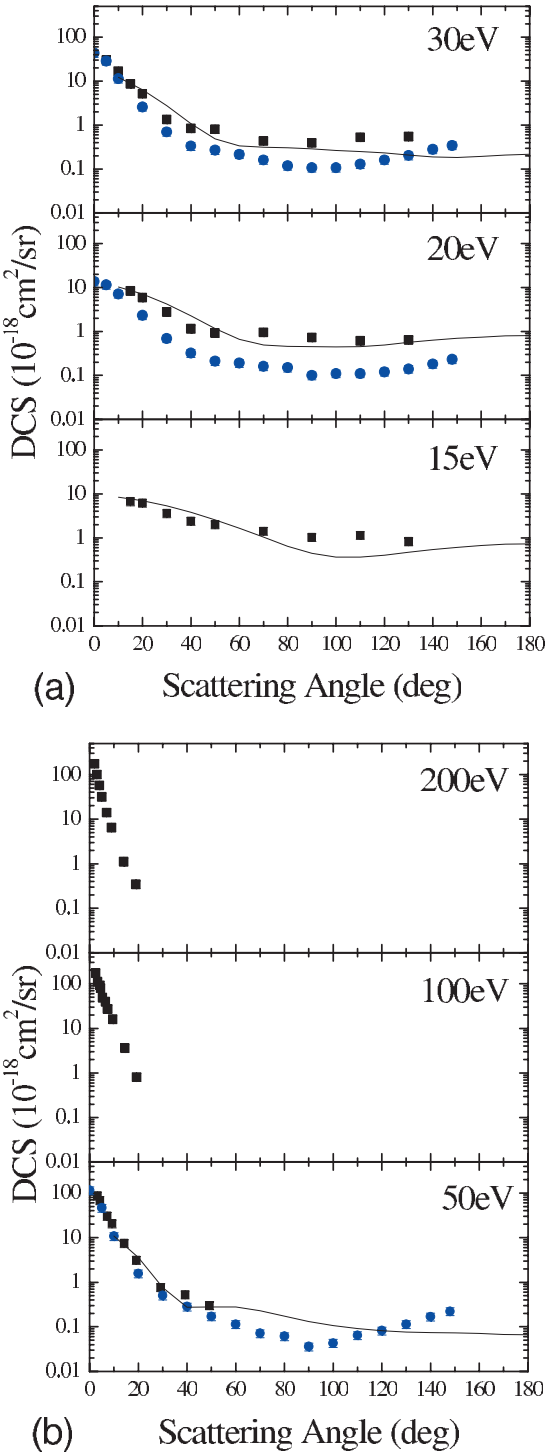

FIG. 2. Differential cross sections for electron impact excitation of the $C\ ^1\Pi$ state at (a) 15, 20, and 30 eV and (b) 50, 100, and 200 eV. The present results (■), those of Marinković *et al.* (Ref. 10) (●) and of Michelin *et al.* (Ref. 14) (—) are plotted.

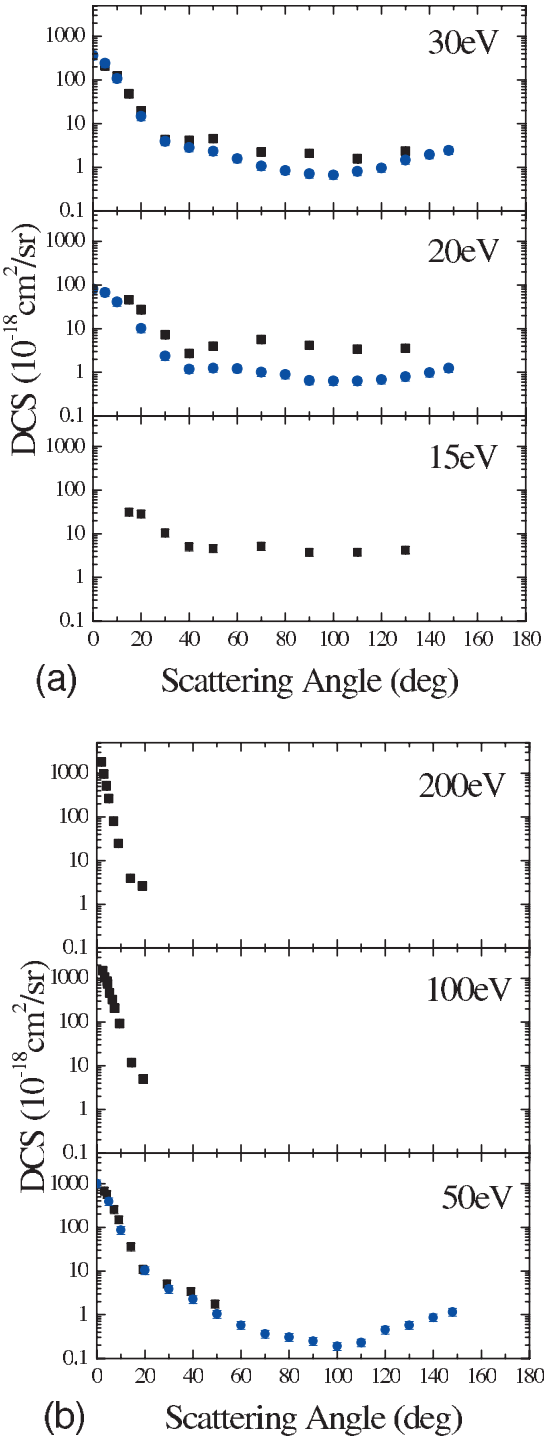

FIG. 3. Differential cross sections for electron impact excitation of the $D\ ^1\Sigma^+$ state at (a) 15, 20, and 30 eV and (b) 50, 100, and 200 eV. The present results (■) and those of Marinković *et al.* (Ref. 10) (●) are plotted.

electron energies as low as 200 eV impact energy, is "somewhat questionable." As a consequence of this we have also included, with our 200 eV data, the 1 keV data of Boechat-Roberty *et al.*[11] and the 2.5 keV data of Zhu *et al.*,[12] in order to obtain estimates for the $C\ ^1\Pi$ and $D\ ^1\Sigma^+$ OOSs (see Fig. 4). This is a valid approach because if the Born approximation is valid all the GOS as a function of K^2 should lie on the one curve, irrespective of the incident electron beam energy.

It is clear from Figs. 4(a) and 4(b) that to within the uncertainties on the respective data sets, for each electronic state, the GOSs from each experiment are in good agreement with one another and so can be fitted by a single function whose form is given by Eqs. (3)–(5). As noted earlier these fits are also shown in Figs. 4(a) and 4(b). The present OOSs are therefore given in Table III. Also listed in Table III are the OOSs for the $C\ ^1\Pi$ and $D\ ^1\Sigma^+$ electronic states from previous measurements[25–29] and theory.[30] We estimate that the uncertainties on our respective OOSs are $\sim \pm 21\%$. Finally, we

TABLE I. Present DCS for electron impact excitation of $C\ ^1\Pi$ state. Errors on the present data are typically ~20%.

θ (deg)	DCS (10^{-18} cm^2/sr)					
	15 eV	20 eV	30 eV	50 eV	100 eV	200 eV
1.95						175
2.5					175	
2.95						101
3.2				86.87		
3.3					112	
3.95						57.36
4.3					93.01	
4.2				68.72		
4.5					79.88	
4.95						31.74
5.0			29.88			
5.3					49.13	
6.5					39.59	
6.95						14.11
7.2				30.63		
7.3					27.04	
7.5					27.43	
8.95						6.50
9.2				20.75		
9.5					16.13	
10.0			16.71			
13.95						1.11
14.2				7.50		
14.5					3.62	
15.0	6.71	8.34	8.68			
18.95						0.35
19.2				3.12		
19.3					0.80	
20.0	6.24	5.90	5.19			
29.2				0.76		
30.0	3.60	2.76	1.34			
39.2				0.53		
40.0	2.41	1.15	0.84			
49.2				0.30		
50.0	2.00	0.92	0.80			
70.0	1.42	0.95	0.44			
90.0	1.03	0.73	0.40			
110.0	1.15	0.61	0.52			
130.0	0.83	0.65	0.55			

note that the procedure outlined above is well-established having been used extensively in studies on other systems (see, e.g., Refs. 31–33).

Finally, estimates of the experimental ICS at each energy can be obtained from Eqs. (3)–(5) using the standard formulae[34]

$$\mathrm{ICS}(E_0) = \frac{4\pi a_0^2}{E_0/R} \int_{K^2_{\min}}^{K^2_{\max}} \frac{G(K^2)}{E/R} d\ln(K^2), \tag{6}$$

with

$$K^2_{\min} = 2\frac{E_0}{R}\left[1 - \frac{E}{2E_0} - \sqrt{1 - \frac{E}{E_0}}\right] \tag{7}$$

and

$$K^2_{\max} = 2\frac{E_0}{R}\left[1 - \frac{E}{2E_0} + \sqrt{1 - \frac{E}{E_0}}\right]. \tag{8}$$

The results from this latter process are listed in Tables IV and V and plotted in Figs. 5(a) and 5(b). We estimate the uncertainties on the present experimental ICS are $\sim \pm 25\%$.

III. THEORY DETAILS

A full description of the BE*f*-scaling approach that we have employed here, to calculate ICS for the $C\ ^1\Pi$ and $D\ ^1\Sigma^+$ states, can be found in Kim,[15] so that only a brief discussion of the more important details need be given here. Note that the scaled (plane-wave) Born cross sections that we used in conjunction with this technique are not only sub-

TABLE II. Present DCS for electron impact excitation of the $D\ ^1\Sigma^+$ state. Errors on the present data are typically ~20%.

θ (deg)	DCS (10^{-18} cm^2/sr)					
	15 eV	20 eV	30 eV	50 eV	100 eV	200 eV
1.95						1824
2.5					1491	
2.95						967
3.2				683		
3.3					1062	
3.95						516
4.3					856	
4.2				571		
4.5					749	
4.95						264
5.0			208			
5.3					462	
6.5					326	
6.95						80.29
7.2				257		
7.3					207	
7.5					207	
8.95						24.84
9.2				150		
9.5					92.94	
10.0			123			
13.95						3.96
14.2				35.98		
14.5					11.87	
15.0	31.61	46.11	48.22			
18.95						2.62
19.2				10.95		
19.3					4.97	
20.0	28.59	27.36	19.63			
29.2				5.11		
30.0	10.57	7.33	4.31			
39.2				3.41		
40.0	5.06	2.73	4.14			
49.2				1.77		
50.0	4.62	4.01	4.55			
70.0	5.21	5.66	2.22			
90.0	3.78	4.16	2.10			
110.0	3.80	3.40	1.58			
130.0	4.26	3.57	2.33			

ject to the approximations in the collision theory part, but also depend on the accuracy of the wave functions used for the initial and final states of the target molecule.

The f-scaled Born cross sections (ICS_f) are given by

$$ICS_f(E_0) = \frac{f_{accur}}{f_{Born}} ICS_{Born}(E_o), \tag{9}$$

where f_{accur} is an accurate OOS value from either accurate wave functions or experiments and f_{Born} is the OOS from the same wave functions used to calculate the unscaled Born cross sections $ICS_{Born}(E_0)$. The f-scaling process has the effect of replacing the wave functions used for ICS_{Born} with accurate wave functions. We note that in the present application the accurate $C\ ^1\Pi$ and $D\ ^1\Sigma^+$ OOSs from Chan *et al.*[25] were used in this process.

The BE-scaled Born cross section (ICS_{BE}) is given by

$$ICS_{BE}(E_0) = \frac{E_0}{(E_0 + B + E)} ICS_{Born}(E_0). \tag{10}$$

This scaling corrects the well-known deficiency of the Born approximation at low E_0, without losing its established validity at high E_0.

If an unscaled $ICS_{Born}(E_0)$ is obtained from poor or marginal wave functions while an accurate OOS is known, then both f-scaling and BE-scaling can be applied to obtain a BEf-scaled Born cross section ($ICS_{BEf}(E_0)$),

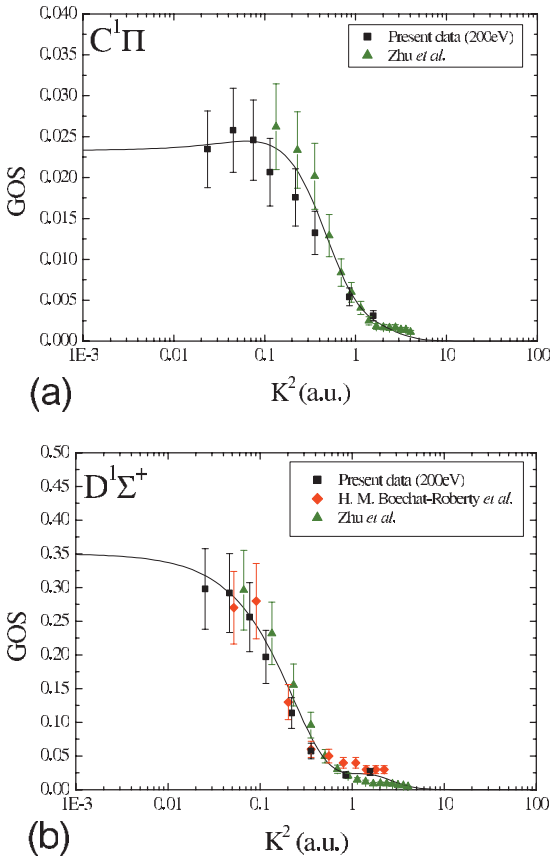

FIG. 4. Representative GOS vs K^2 plots at E=200 eV, for the $X\ ^1\Sigma^+ \rightarrow C\ ^1\Pi$ excitation (a) and the $X\ ^1\Sigma^+ \rightarrow D\ ^1\Sigma^+$ excitation (b). The present data (■) and those of Boechat-Roberty *et al.* (Ref. 11) (◆) and Zhu *et al.* (Ref. 12) (▲) are shown, as are the fits, using Eqs. (3)–(5), to those data (—).

$$\mathrm{ICS}_{\mathrm{BE}f}(E_0) = \frac{f_{\mathrm{accur}} E_0}{f_{\mathrm{Born}}(E_0 + B + E)} \mathrm{ICS}_{\mathrm{Born}}(E_0). \qquad (11)$$

The current calculated $\mathrm{ICS}_{\mathrm{BE}f}(E_0)$ integral cross sections are listed for the *C*- and *D*-states in Tables IV and V and compared against our experimental ICS, and those derived from the measurements of Boechat-Roberty *et al.*[11] and Zhu *et al.*,[12] in Figs. 5(a) and 5(b).

TABLE III. Optical oscillator strengths for the $C\ ^1\Pi$ and $D\ ^1\Sigma^+$ electronic states from our analysis and a selection of the available earlier results.

	$C\ ^1\Pi$	$D\ ^1\Sigma^+$
Experiment		
Present work	0.0233	0.350
W. F. Chan *et al.*[a] [HR dipole (e,e′)]	0.0245	0.376
Lee and Suto[b] (photoabsortion)	0.0253	0.378
Huebner *et al.*[c] (electron impact)	0.0285	0.352
Rabalais *et al.*[d] (photoabsorption)	0.007	0.36
Zelikoff *et al.*[e] (photoabsorption)	0.0211	0.367
Theory		
Chutjian and Segal[f]	0.029	0.77

[a]Reference 25.
[b]Reference 26.
[c]Reference 27.
[d]Reference 28.
[e]Reference 29.
[f]Reference 30.

TABLE IV. Present ICS for electron impact excitation of the $C\ ^1\Pi$ state. Errors on the present data are typically ~25%. The value of Zhu *et al.* is calculated from their GOS data.

E_0 (eV)	ICS (10^{-18} cm^2) BE*f*	Present work	Zhu *et al.*[a]
8.5	0.00		
10	4.85		
12	7.09		
15	8.82	19.99	
20	9.97	15.21	
30	10.20	13.28	
40	9.69		
50	9.06	8.93	
60	8.45		
70	7.89		
80	7.40		
90	6.96		
100	6.57	6.60	
150	5.14		
200	4.24	3.91	
300	3.17		
400	2.55		
500	2.14		
600	1.86		
700	1.64		
800	1.47		
900	1.34		
1000	1.23		
1500	0.87		
2000	0.68		
2500	0.57		0.62
3000	0.48		
4000	0.38		
5000	0.31		

[a]Reference 12.

The numerical uncertainty in the plane-wave Born cross sections would probably be <1%; however, the final uncertainty on our BE*f*-scaled results will be largely determined by the accuracy of the OOS used in the *f*-scaling process. Such an uncertainty would typically be in the range 5%–10%.[25]

Finally, we note that in the present calculations we chose the theoretical work of Peyerimhoff and Buenker[35] to generate the unscaled Born cross sections. While their optical oscillator strength values do not agree with those from the accurate dipole (e,e′) experiments of Chan *et al.*[25] (see Table III), the BE*f*-scaled Born cross sections in principle correct for this.

IV. RESULTS AND DISCUSSION

In Tables I and II and Figs. 2 and 3 we list and plot the present DCSs for electron impact excitation of the $C\ ^1\Pi$ and $D\ ^1\Sigma^+$ electronic states of N_2O. Also included in Figs. 2 and 3, where possible, are the earlier data from Marinković *et al.*[10] and, for the $C\ ^1\Pi$ state, the SVIM calculation results from Michelin *et al.*[13,14] There are several features common to both Figs. 2 and 3. They include that for both states the

TABLE V. Present ICS for electron impact excitation of the $D\ ^1\Sigma^+$ state. Errors on the present data are typically ~25%. The values of Zhu *et al.* and Boechat-Roberty *et al.* are calculated from their GOS data.

E_0 (eV)	ICS (10^{-18} cm^2) BE*f*	Present work	Boechat-Roberty *et al.*[a]	Zhu *et al.*[b]
9.6	0.00			
10	5.78			
12	17.43			
15	28.82	73.42		
20	40.27	76.24		
30	50.17	60.57		
40	52.94			
50	52.98	55.64		
60	51.87			
70	50.30			
80	48.56			
90	46.80			
100	45.08	49.87		
150	37.79			
200	32.49	32.64		
300	25.53			
400	21.18			
500	18.18			
600	15.99			
700	14.31			
800	12.97			
900	11.88			
1000	10.98		11.75	
1500	8.04			
2000	6.40			
2500	5.35			7.16
3000	4.62			
4000	3.65			
5000	3.03			

[a]Reference 11.
[b]Reference 12.

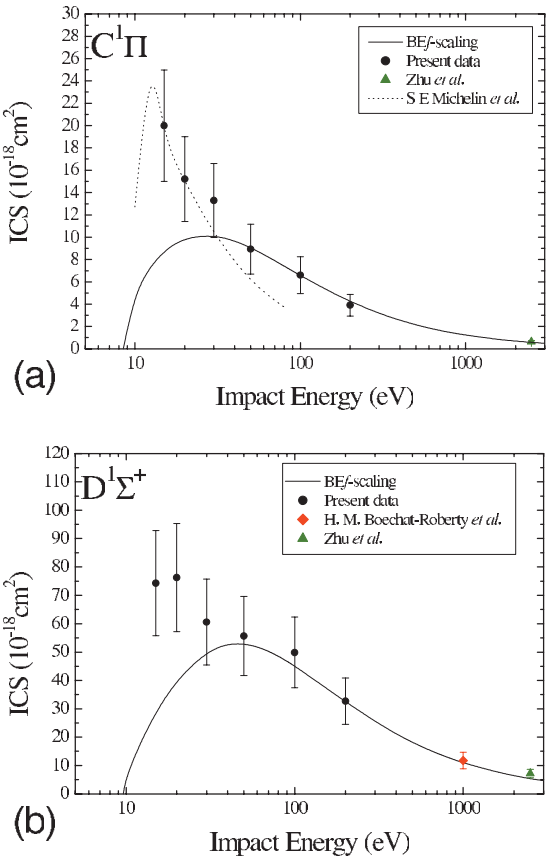

FIG. 5. ICS for electron impact excitation of the $C\ ^1\Pi$ (a) and $D\ ^1\Sigma^+$ (b) states. The present data (●) and those of Boechat-Roberty *et al.* (Ref. 11) (◆) and Zhu *et al.* (Ref. 12) (▲) are shown, as well as our BE*f*-scaling results and the results from the calculation of Michelin *et al.* (Ref. 14)

DCSs are strongly peaked at the more forward electron scattering angles, with the degree of this "forward peaking" increasing as the incident electron energy is increased. This behavior is consistent with N_2O possessing both an important (in terms of its magnitude) dipole polarisability[5] and a permanent, although relatively small, dipole moment.[7] We had previously seen in our study of electron impact excitation of the electronic states in NO[36,37] [μ_{NO}=0.157 D (Ref. 36)], that a small permanent dipole moment can have a dramatic effect on the scattering process and the behavior observed in Figs. 2 and 3 is consistent with that earlier result. It is also clear from Figs. 2 and 3 that at 20, 30, and 50 eV, again for both the $C\ ^1\Pi$ and $D\ ^1\Sigma^+$ states, the original DCS of Marinković *et al.*[10] tends to somewhat underestimate the magnitude of the DCS for electron scattering angles greater than about 20°. If you consider the *y*-axis on Figs. 2 and 3, then it is immediately apparent that the dynamical range of these DCSs can vary by 3–4 orders of magnitude over the scattered electron angular range considered. This observation suggests that these are tough experiments, in terms of maintaining system stability and apparatus response functions over the sometimes extended data collection periods, representing a significant challenge to experimentalists. Finally, in Fig. 2, we can compare both sets of data to the theoretical SVIM results.[13,14] It is apparent from Fig. 2 that the present data and the computation of Michelin *et al.* are in rather good agreement, at the incident electron energies where a direct comparison is possible. However, we suspect that, at least in part, this high level of agreement is somewhat fortuitous. The basis set employed by Michelin *et al.*[13,14] led to a calculated dipole moment of 0.68 D, which is some four times larger than that from experiment. As the dipole moment is one indicator for the efficacy of the structure part of a calculation, this poor level of agreement between their calculated dipole moment and the experimental value suggests an important limitation with their target description. As such, it follows that the agreement we find at the DCS level for the $C\ ^1\Pi$ state might be a little fortuitous.

In Fig. 4 we show the least-squares[21] fits to our $C\ ^1\Pi$ and $D\ ^1\Sigma^+$ GOS versus K^2 data (see Sec. II), and the relevant data from Boechat-Roberty *et al.*[11] and Zhu *et al.*[12] We would characterize these fits to the available data as being very good, thereby giving us confidence in the respective extrapolations to K^2=0 leading to our determination of the OOS values for each state. Those OOS values are tabulated in Table III, along with the results from previous measurements[25–29] and an earlier calculation.[30] Considering Table III in more detail, we find the present $C\ ^1\Pi$ OOS is in very good agreement, to within our error of measurement

(~ ± 21%), with the dipole (e,e′) result of Chan *et al.*[25] and the photoabsorption data of Lee and Suto.[26] A similar level of agreement for the OOS of the $D\ ^1\Sigma^+$ state, between the present result and those previous investigations,[25,26] is also found. Agreement with the theoretical $C\ ^1\Pi$ OOS of Chutjian and Segal[30] is also satisfactory, but this calculation overestimates the magnitude of the $D\ ^1\Sigma^+$ OOS by about a factor of 2. The very good agreement we find between our respective OOSs and those from Chan *et al.*,[25] give us confidence in the validity of using the OOSs from Chan *et al.* in our BE*f*-scaling calculations (see below).

In Tables IV and V and Figs. 5(a) and 5(b) we now present our $C\ ^1\Pi$ and $D\ ^1\Sigma^+$ ICSs. Also shown in Tables IV and V and these figures are our calculated BE*f*-scaling ICS, from threshold to 5000 eV, and ICS we have derived from the work of Boechat-Roberty *et al.*[11] and Zhu *et al.*[12] Our procedures for determining the experimental ICS can be found in Sec. II, while a brief description of the BE*f*-scaling approach was provided in Sec. III. Similar to what we found at the DCS level, there are also common features for both the $C\ ^1\Pi$ and $D\ ^1\Sigma^+$ ICSs. In particular, at energies greater than about 30 eV, to within the uncertainty on our ICS (~25%), the present BE*f*-scaling results are in very good accord with the current measured ICS and the ICS we have derived from Boechat-Roberty *et al.* and Zhu *et al.* Below 30 eV, however, the present measured ICS are significantly stronger in magnitude than the corresponding results from our BE*f*-scaling calculation. We believe there could be two factors to explain this discrepancy. First, spectroscopic calculations from Hopper[38] and Cubric *et al.*[39] suggest the existence of a $d\ ^3\Pi$ state at 8.3 eV threshold energy (i.e., nearly degenerate with the $C\ ^1\Pi$ state) and a $2\ ^3\Pi$ state at 9.6 eV threshold energy (i.e., nearly degenerate with the $D\ ^1\Sigma^+$ state). As the dominant population mechanism of those triplet states would be through electron exchange (the ground electronic state of N_2O is a singlet[39]), and as exchange cross sections generally have a large peak near-threshold before tapering off in magnitude as the incident electron energy increases, the low energy behavior in Figs. 5(a) and 5(b) is consistent with there being some unresolved contribution from these $d\ ^3\Pi$ and $2\ ^3\Pi$ states to the respective $C\ ^1\Pi$ and $D\ ^1\Sigma^+$ electronic states. The second possible explanation, for the low energy behavior observed in Figs. 5(a) and 5(b), relies on the existence of a broad shape ($^2\Sigma$) resonance, centered at around 13 eV, as predicted by the calculation of Michelin *et al.*[13] Indeed the $C\ ^1\Pi$ ICS of Michelin *et al.*[13] [see Fig. 5(a)] is in very good agreement with the present measured ICS for energies less than about 30 eV, consistent with this resonance decaying into the $C\ ^1\Pi$ electronic state. Unfortunately this second possible explanation is controversial, as an independent Schwinger multichannel calculation from da Costa and Bettega[40] could not confirm the existence of this resonance. Furthermore the grand TCS experiments of Szmytkowski *et al.*[41] also show no structure at this energy, although we admit that the TCS might not be the most sensitive metric on which to base a judgment on this point. Certainly more theory is needed to address this point definitively. Nonetheless, on balance, at this time we believe that the most likely explanation for the discrepancies between our BE*f*-scaling ICS and measured ICS, at low energies, for the $C\ ^1\Pi$ and $D\ ^1\Sigma^+$ electronic states, is due to triplet contamination at these lower energies.

Finally let us compare the 50 eV $C\ ^1\Pi$ ICS of N_2O with the corresponding $^1\Pi_u$ ICS in CO_2[8], and the 50 eV $D\ ^1\Sigma^+$ ICS of N_2O with the corresponding $^1\Sigma_u^+$ ICS of CO_2[8]. Note that we have chosen these energies as any possible triplet contamination to the N_2O cross sections and any possible $^2\Sigma$-resonance contribution to the N_2O cross sections will be minimal. However, we could have just as easily picked other energies and the discussion that follows would still be valid. We find that the $C\ ^1\Pi$ ICS of N_2O is greater in magnitude than the $^1\Pi_u$ ICS of CO_2 by a factor of ~1.5, while the $D\ ^1\Sigma^+$ ICS is greater than the ICS for the $^1\Sigma_u^+$ electronic state by a factor of 3.3. As both N_2O and CO_2 are linear triatomics, as both are isoelectronic and as both have similar dipole polarizabilities, we believe the differences noted above simply reflect, to a large degree, that N_2O has a permanent dipole moment while CO_2 does not.

V. CONCLUSIONS

We have reported new DCS measurements for electron impact excitation of the $C\ ^1\Pi$ and $D\ ^1\Sigma^+$ electronic states in nitrous oxide. Agreement with earlier data of Marinković *et al.*[10] was found to be fair, although agreement with the SVIM calculation of Michelin *et al.*[13,14] for the $C\ ^1\Pi$ state was remarkably good. Optical oscillator strengths determined from this study were found to be in very good agreement with a previous accurate dipole (e,e′) study[25] and a photoabsorption study.[26] The present experimental $C\ ^1\Pi$ and $D\ ^1\Sigma^+$ ICS, for energies greater than ~30 eV, and ICS derived from earlier work[11,12] were found to be in very good accord with our respective BE*f*-scaling results. At lower energies, the comparison was complicated by a probable triplet-state contribution to our energy loss spectra. However, we would still suggest that the current BE*f*-scaling results provide a useful and accurate contribution to the database needed for scientists wishing to model, e.g., plasma processes in which N_2O is a constituent. Finally we note the important roles played by both the dipole polarizability and dipole moment of N_2O in the excitation dynamics of these electronic states.

ACKNOWLEDGMENTS

This work was conducted under the support of the Japanese Ministry of Education, Sport, Culture and Technology. One of us (H.K.) also acknowledges the Japan Society for the Promotion of Science (JSPS) for their fellowships as grants-in-aid for scientific research. Two of us (L.C. and M.J.B.) were supported in part by the Australian Research Council through its Centres of Excellence Program.

[1] R. P. Waye, *Chemistry of Atmospheres*, 2nd ed. (Oxford Science Publications, Oxford, 1991).
[2] M. Kitajima, Y. Sakamoto, R. J. Gulley, M. Hoshino, J. C. Gibson, H. Tanaka, and S. J. Buckman, J. Phys. B **33**, 1687 (2000).
[3] L. M. Ziurys, A. J. Apponi, J. M. Hollis, and L. E. Snyder, Astrophys. J. **436**, L181 (1994).
[4] J. Elsila, L. J. Allamandola, and S. A. Sandford, Astrophys. J. **479**, 818 (1997).

[5] *CRC Handbook of Chemistry and Physics*, 76th ed., edited by D. R. Lide (CRC, Boca Raton, Fl, 1995).
[6] G. R. Alms, A. K. Burnham, and W. H. Flygar, J. Chem. Phys. **63**, 3321 (1975).
[7] H. Jalink, D. H. Parker, and S. Stolte, J. Mol. Spectrosc. **121**, 236 (1987).
[8] H. Kawahara, H. Kato, M. Hoshino, H. Tanaka, L. Campbell, and M. J. Brunger, J. Phys. B **41**, 085203 (2008).
[9] M. Allan and T. Skalický, J. Phys. B **36**, 3397 (2003).
[10] B. Marinković, R. Panajotović, Z. D. Pesić, D. M. Filipović, Z. Felfli, and A. Z. Msezane, J. Phys. B **32**, 1949 (1999).
[11] H. M. Boechat-Roberty, M. L. M. Rocco, C. A. Lucas, and G. G. B. de Souza, J. Phys. B **33**, 4525 (2000).
[12] L.-F. Zhu, J.-M. Sun, and K.-Z. Xu, *Book of Abstracts*, Vol. 25, ICPEAC, edited by J. Anton, R. Moshammer, C. -D. Schröter, and J. Ullrich, (University of Freiburg Press, Freiburg, Germany, 2007).
[13] S. E. Michelin, T. Kroin, and M. T. Lee, J. Phys. B **29**, 2115 (1996).
[14] S. E. Michelin, T. Kroin, and M. T. Lee, J. Phys. B **29**, 4319 (1996).
[15] Y.-K. Kim, J. Chem. Phys. **126**, 064305 (2007).
[16] H. Tanaka, L. Boesten, D. Matsunaga, and T. Kubo, J. Phys. B **21**, 1255 (1988).
[17] J. C. Nickel, P. W. Zetner, G. Shen, and S. Trajmar, J. Phys. E **22**, 730 (1989).
[18] L. Boesten and H. Tanaka, At. Data Nucl. Data Tables **52**, 25 (1992).
[19] H. Kato, H. Kawahara, M. Hoshino, H. Tanaka, M. J. Brunger, and Y.-K. Kim, J. Chem. Phys. **126**, 064307 (2007).
[20] H. Tanaka, T. Ishikawa, T. Masai, T. Sagara, L. Boesten, M. Takekawa, Y. Itikawa, and M. Kimura, Phys. Rev. A **57**, 1798 (1998).
[21] L. Vriens, Phys. Rev. **160**, 100 (1967).
[22] E. N. Lassettre, J. Chem. Phys. **43**, 4479 (1965).
[23] A. R. P. Rau and U. Fano, Phys. Rev. **162**, 68 (1967).
[24] B. R. Lewis, Phys. Rev. A **78**, 026701 (2008).
[25] W. F. Chan, G. Cooper, and C. E. Brion, Chem. Phys. **180**, 77 (1994).
[26] L. C. Lee and M. Suto, J. Chem. Phys. **80**, 4718 (1984).
[27] R. H. Huebner, R. J. Celotta, S. R. Mielczarek, and C. E. Kuyatt, J. Chem. Phys. **63**, 4490 (1975).
[28] J. W. Rabalais, J. M. McDonald, V. Scherr, and S. P. McGlynn, Chem. Rev. (Washington, D.C.) **71**, 73 (1971).
[29] M. Zelikoff, K. Watanabe, and E. C. Y. Inn, J. Chem. Phys. **21**, 1643 (1953).
[30] A. Chutjian and G. A. Segal, J. Chem. Phys. **57**, 3069 (1972).
[31] R. Muller-Fiedler, K. Jung, and H. Ehrhardt, J. Phys. B **19**, 1211 (1986).
[32] A. Lahmam-Bennani, M. Cherid, and A. Duguet, J. Phys. B **20**, 2531 (1987).
[33] J. Mitroy, Phys. Rev. A **35**, 4434 (1987).
[34] B. H. Bransden and C. J. Joachain, *Physics of Atoms and Molecules* (Longman, London, 1983).
[35] S. D. Peyerimhoff and R. J. Buenker, J. Chem. Phys. **49**, 2473 (1968).
[36] M. J. Brunger, L. Campbell, D. C. Cartwright, A. G. Middleton, B. Mojarrabi, and P. J. O. Teubner, J. Phys. B **33**, 783 (2000).
[37] M. J. Brunger, L. Campbell, D. C. Cartwright, A. G. Middleton, B. Mojarrabi, and P. J. O. Teubner, J. Phys. B **33**, 809 (2000).
[38] D. G. Hopper, J. Chem. Phys. **80**, 4290 (1984).
[39] D. Cubric, D. Cvejanović, J. Jureta, S. Cvejanović, P. Hammond, G. C. King, and F. H. Read, J. Phys. B **19**, 4225 (1986).
[40] S. M. S. da Costa and M. H. F. Bettega, Eur. Phys. J. D **3**, 67 (1998).
[41] C. Szmytkowski, G. Karwasz, and K. Maciag, Chem. Phys. Lett. **107**, 481 (1984).